

4-Stroke Port Injected Turbocharged Snowmobile Design

Clean Snowmobile Challenge 2014 Design paper

Copyright © 2012 SAE International

ABSTRACT

With growing concerns regarding emissions controls with recreational vehicles such as the snowmobile, Team QUIETS has decided to take on the challenge of modifying and improving the image of the snowmobile. The snowmobile used for the research is a 600 ACE 4 stroke engine from BRP. Modifications to improve engine mileage and the reduction of sound and exhaust emissions include the implementation of a turbocharger, a catalytic converter, a redesigned exhaust system, EGR system and a new engine control system. All these modifications made to the engine will allow the snowmobile to have excellent fuel efficiency, reduced sound and exhaust emissions while maintaining and even surpassing the stock engine power output. The modified snowmobile now has a peak power output of 85 horse power (HP) and 76 foot pounds (ft-lbs) of torque at 7200 RPM. The resulting global decibel level of the snowmobile in perfect trail conditions is now at 71 decibels (dB(A)), a 1 dB(A) reduction compared to the stock decibel level of 72 dB(A). This student club is a great example of what a group of 16 people with common goals can accomplish.

INTRODUCTION

Team QUIETS is very proud to present our submission for the 2014 Clean Snowmobile Challenge. This year we are continuing with a turbo charged 4-stroke engine design; we believe that this will allow us to achieve the great handling and acceleration characteristics we enjoyed with the two-stroke engine, all the while reducing emissions and noise to more competitive levels. We also believe that this year's project is considerably more economically viable than its predecessors, as it relies more on stock components and high-value modifications. We have accomplished a lot in a relatively short time, and hope that our efforts will pay off at the CSC 2013.

ETS – CSC SNOWMOBILE DESIGN AND MODIFICATIONS

Snowmobile Engine Comparison and Selection

The snowmobile engine selection had to be according to our objectives. We are looking for a small light engine block with good fuel economy and the reliability to withstand harsh engine calibration. With the help of forums on behalf of the FCMQ (Federation of Snowmobile Clubs of Quebec), we were able to determine the needs of the rider. Environmental issues are not a big concern in the region of Quebec, the main attraction from the buyer's point of view is power and fuel economy. Usually, these two qualities do not go hand in hand, but with the use of small turbo charged engine block with available table switching modes, buyers could get a good compromise on both desires. Theoretically, a 600 Ace turbo charged will have a better fuel economy than its new little brother, the 900 Ace, which is a naturally aspired engine. Going for small turbo charged engine pushes the snowmobile industry to follow the automotive industry where we can witness a rising amount of models available with smaller turbo charged engine blocks with better fuel economy.

Table 1 - Snowmobile Comparison

	900 Ace	Etec	600 Ace Turbo
Displacement	900 cc	600 cc	600 cc
Stroke	4 Stroke	2 Stroke	4 Stroke
Hp	90	121	85
Fuel Consumption	23 mpg	21 mpg	24 mpg

Engine Control and Calibration

For the 2014 edition CSC challenge we upgraded our engine management computer (EMC) to a Megasquirt Pro. We made that decision to solve some of the weaknesses of the Megasquirt 3. First of all, the Megasquirt Pro's hardware offers a much more robust solution. The new ECM is much smaller than the previous one and is fully waterproof. Secondly, the transition from a Megasquirt 3 to a Megasquirt Pro is fairly easy since the firmware changes don't affect the engine management and the I/O are identical. Finally, considering our previous experiences with the Megasquirt series the upgrade was the natural thing to do.

The Megasquirt Pro is the most advanced version of the Megasquirt series, providing almost all of the features found in other engine management computers for a fraction of the price. It is designed to be easy for anyone to implement and has a fairly large community for support as well as in-depth documentation available on the MS3 web site. Above all, the availability of (older) source code and schematics allows us to retain some of the flexibility we enjoyed with the MotoTron/MotoHawk system. With the new version of the EMC we are now confident that our concept can resist the toughest winter conditions.

We believe that completely replacing the snowmobile's EMS gives us an important degree of flexibility in our projects and this year was no different. The unfortunate consequence is that, for the first year at least, one of the largest and most important tasks for our team is the calibration of the engine. This year, we had the added challenge of getting engine to run up to its maximum potential RPM which is 7200 RPM. The engine calibration had to be perfect in order to avoid damaging the engine the high amount of heat caused by the turbo. Our task was greatly assisted by the auto-tuning feature provided with the Megasquirt's tuning software, as well as embedded closed loop functionality as seen in figure 1.

	500	800	1100	1400	2000	2600	3100	3700	4300	4900	5400	6000
a	11.0	11.0	11.0	11.0	11.0	11.0	11.0	11.0	11.0	11.0	11.0	11.0
f	11.7	11.6	11.6	11.6	11.6	11.6	11.5	11.5	11.5	11.4	11.4	11.4
r	12.3	12.3	12.3	12.2	12.2	12.1	12.1	12.0	12.0	11.8	11.8	11.8
l	12.9	12.8	12.8	12.7	12.7	12.6	12.5	12.5	12.5	12.2	12.2	12.2
o	13.0	12.9	12.9	12.8	12.8	12.7	12.6	12.5	12.5	12.5	12.3	12.3
a	13.0	12.9	12.9	12.8	12.8	12.7	12.6	12.5	12.5	12.5	12.5	12.4
d	13.0	13.0	13.1	13.0	13.0	12.9	13.0	12.5	12.5	12.5	12.5	12.5
t	13.4	13.4	13.9	13.7	13.6	13.6	13.1	12.7	12.6	12.6	12.6	12.6
1	13.6	14.1	14.3	14.2	14.1	13.9	13.4	12.9	12.8	12.7	12.6	12.6
5	13.5	14.0	14.7	14.6	14.5	14.3	13.6	13.0	12.9	12.8	12.7	12.6
4	13.4	13.9	15.5	15.5	15.4	14.9	14.1	13.0	12.9	12.8	12.7	12.7
3	13.0	13.5	16.0	16.0	16.0	14.9	14.3	13.2	13.1	13.2	13.1	13.0

Figure 1 - AFR Table (Engine Load vs RPM)

As an added precaution, the spark plugs were replaced with "colder" variants, in order to reduce the chances of detonation and pre-ignition brought on from the added spark advance.

Engine Calibration Strategy

Running the engine at a stoichiometric ratio of 1 for Lambda is ideal for maximum efficiency and emission's control. But to maximize fuel economy, a lean combustion is required. To save on fuel, the programmed closed loop AFR target during cruising speed will rise to 1.02, meaning that between 5000 and 6000 RPM and between a TPS position of 15 to 30%, the engine will be running on a lean air/fuel mixture.

The programmed AFR value was calculated with the help of the specific fuel consumption (SFC) in g/KW-hr represented by the equation (1).

$$SFC = \frac{\dot{m}}{P} \quad (1)$$

Where m is the fuel flow in g/h and P is the engine's power output in kW. On a bench test, while keeping the engine at a constant speed and load, it is possible to witness the variation of the SFC by changing the AFR. Testing various ratios will trace a curve on a graph on figure 2.

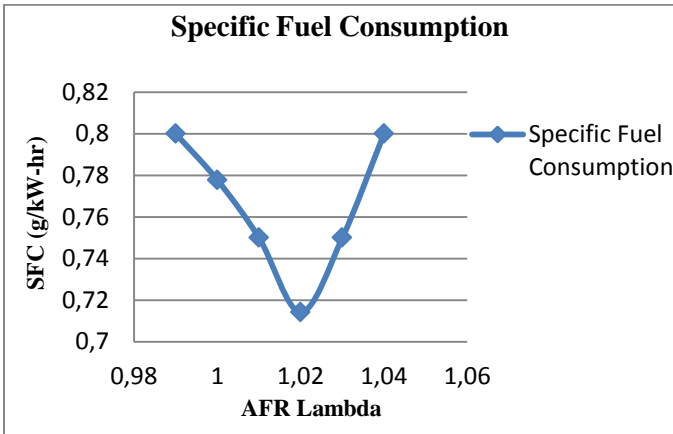


Figure 2 - Engine's Specific Fuel Consumption

So by following this curve, we can establish the correct AFR for each operation point running with a lean air/fuel mixture.

Engine Emission's Control

Regarding emissions found in exhaust gases, only three types of particles really cause a problem for 4 stroke engine. According EPA standards, our engine should pass a 5-mode resulting in an E-score greater or equal to 100. According to the following formula:

$$E = \left(1 - \frac{(HC + NO_x) - 15}{150}\right) * 100 + \left(1 + \frac{CO}{400}\right) * 100 \quad (2)$$

The compilation of the measured brake specific emissions (g/Kw-hr) of HC, NOx and CO will require a score greater than 100. To accomplish this goal our team has opted for implement two types of emissions control systems. Since most of engine's running point aim for a stoichiometric efficiency ($\lambda=1$), a good majority of the exhaust gas emissions can be treated with the help of three way catalyst. A catalyst composed of a stainless steel casing and of a stainless steel substrate from the company Aristo and Emitec coated layers of platinum, rhodium and palladium. This single bed three-way catalytic converter system offers conversion efficiency between 80-95% depending of the engine's operating conditions and air/fuel ratio as seen in the table below.

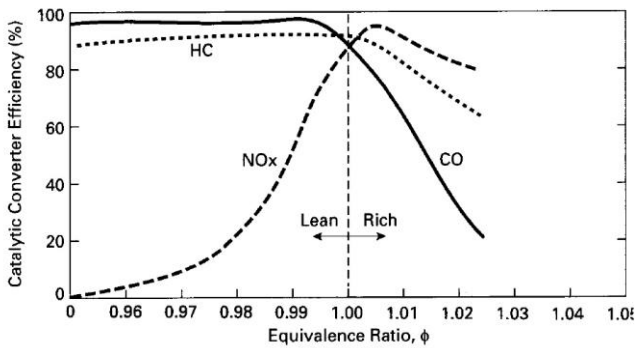


Figure 3 - Catalytic Converter Efficiency vs Air/Fuel Ratio

By referring our engine calibration to the figure 3, we can notice that a maximum of the catalytic converter's efficiency is achieved at an air/fuel ratio of $\phi=1$. Going back to our engine control from the previous section, our fuel/air ratio (ϕ) will drops to 0.98 during cruising speeds of 45 mph in order to improve the snowmobile's fuel efficiency. But while saving on fuel, our engine's emissions were altered. As seen on figure y, decreasing the value of ϕ causes a reduction in HC and CO particles, but an increase in NOx.

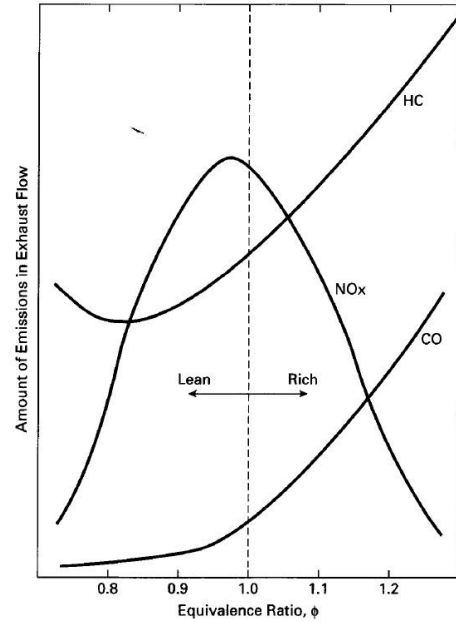


Figure 4 - Amount of Emissions in Exhaust Gases vs Air/Fuel Ratio

Not only that, but the lean air/fuel mixture reduces the efficiency of the catalytic converter. A test was run to show the effects of running an engine lean on fuel on NOx formation. The tests were carried out at an engine speed of 3500 RPM and with a 30% throttle position opening.

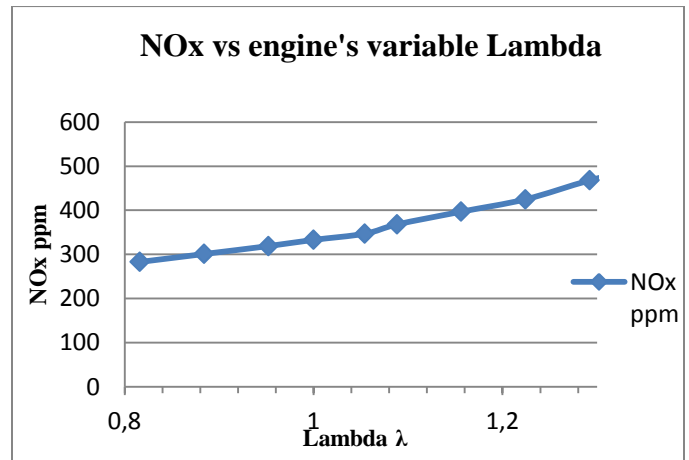


Figure 5 - NOx ppm vs Engine Lambda of operation (at 3500 RPM at 30% TPS)

By observing the results illustrated on the figure 5, we can conclude that a lean running engine produces a non-negligible augmentation of NOx. As seen in figure 1, the catalytic converter will still be efficient for HC and CO particles with a lean burning engine but conversion efficiency for NOx will drop drastically. Looking at NOx formation, we can identify three sources contributing to its formation. The first and major source of NOx formation is due to heat peaks in the combustion chamber, the second source is due to the reaction of nitrogen with hydrocarbon radicals. The last source of NOx

formation is due to the nitrogen found in the fuel itself. Since the heat peaks in the combustion chamber is considered the most significant source for NO_x formation, a consideration was taken to eliminate the two other sources and working on reducing the flame temperature of the combustion. By looking at the figure 6 illustrating the Zeldovich NO_x formation model, we can observe the direct link to flame temperature and NO_x formation rate.

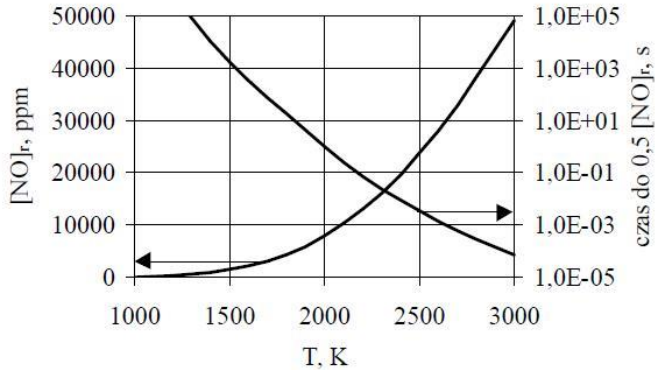
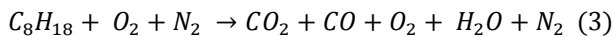


Figure 6 - NO_x ppm vs flame temperature (NO_x formation according to the Zeldovich model)

With such a comparison, the inevitable solution for this problem would be to implement an EGR system in order to reduce the combustion flame temperature. By re-circulating a certain percentage of the exhaust gases, the quantity of oxygen available for the combustion is reduced and replaced with inert gases such as CO and CO₂. To be able to get the approximate quantity required, a comparison method is used to calculate the amount of energy on the reactive side of the combustion chemical equation versus the amount of energy on the product side of the equation.



By using the first rule of thermodynamics, a balanced energy equation can be established. For this comparison method, we consider that there is no work exchanged (W), no kinetic energy (Ek), no potential energy (Ep) and no heat exchanged with surrounding environments (combustion chamber).

$$Q - W = \Delta E = \Delta H + \Delta E_c + \Delta E_p \quad (4)$$

$$\Delta E = \Delta H \quad (5)$$

$$\Delta E = H_{product} - H_{reactive} \quad (6)$$

What we have left is the difference between the enthalpy of the reactive and the enthalpy of the products. In other words, the enthalpy of the products is equal to the enthalpy of the reactive.

$$H_{product} = H_{reactive} \text{ (Units kJ/kmol)} \quad (7)$$

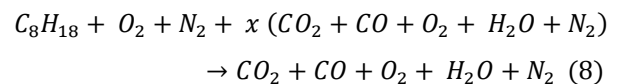
$$\begin{aligned} & [\sum np (h^{\circ f} + (h - h^{\circ}))]_{product} \\ & = \sum nr (h^{\circ f} + (h - h^{\circ}))_{reactive} \end{aligned}$$

We can now work with the equation above to compare the enthalpy by estimating a combustion flame temperature for the reactive. We have h^{°f} representing the formation enthalpy of the molecules, h represents the enthalpy of a molecule at a known temperature and h[°] represents the enthalpy at a reference temperature. By starting with a flame temperature of 1600 K, we can assume that the actual temperature will be much higher, therefore, it is possible to iterate to a higher flame temperature until the enthalpy of the products is equal to the enthalpy of the reactive. This temperature will give us the peak temperature of the combustion for a given combustion formula.

Table 2 - Theoretical Adiabatic Fuel Temperature (K)

TPS (%)	40	1620	1680	1600	1580	1560	1560
	35	1620	1680	1600	1600	1560	1560
	30	1620	1660	1580	1580	1560	1560
	25	1620	1660	1580	1580	1560	
	20	1600	1640				
	15	1600					
	3250	3750	4500	4750	5250	5500	
	RPM						

In table 2, we can find the theoretical adiabatic flame temperature of combustion for the operating cells of the EGR valve. With these temperatures, we can now fix a reduction objective which in our case is 200K. The new combustion equation with re-circulated gases is as described below with x representing the percentage of gases re-circulated.



The actual quantity of exhaust gases re-circulated is determined with the difference in pressure between the intake of the EGR valve and the out port, and the EGR valve position. By using Bernoulli's equation of energy, we can isolate the fluid speed variable which will vary with the valve's position.

$$Z_1 + \frac{P_1}{\gamma} + \frac{v_1^2}{2g} + H_p - H_m - H_L = Z_2 + \frac{p_2}{\gamma} + \frac{v_2^2}{2g} \quad (9)$$

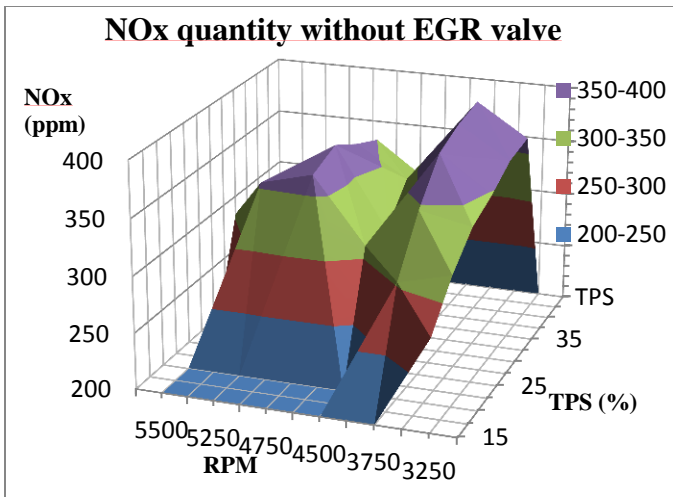


Figure 7 - NOx Quantity with no EGR Valve

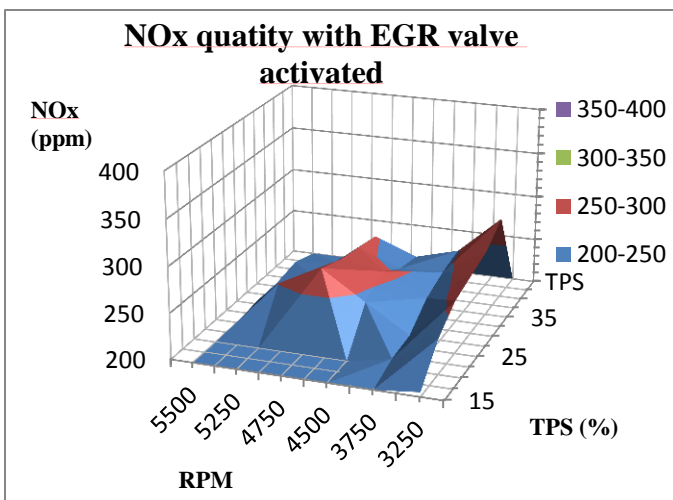


Figure 8 - NOx Quantity with Active EGR Valve

By comparing figure 7 and 8, the effects of the EGR valve on NOx have been proven very effective. The achieved global NOx reduction of 23% in the EGR's operating range proves that the reduction in the flame temperature is directly linked to the reduction of NOx.

Following the emissions data collection, a rise in HC particles and a loss in power were noticed. The air fuel ratio also dropped resulting in a rich combustion. To explain these variances, the following equation representing the flame's front speed shows the effects of re-circulated gases.

$$S_L(x_b) = S_L * (1 - 2.06 * x_b^{0.77}) \quad (10)$$

Where S_L is the flame speed and x_b is the percentage of re-circulated gases. With a greater quantity of re-circulated gases, the flame speed reduces. To compensate, more spark advance is needed to allow more complete flame propagation and to be able to harvest the maximum amount of power from the fuel.

Acoustics and Noise Reduction

2014 Exhaust Design

This section examines more thoroughly the thought process behind the design of the new exhaust system. For the most part, this year's product is based on last year's concept. Since the previous exhaust yield good improvement over stock, it served as a base for the new system.

The casing of the new muffler is very similar to the previous one. As a matter of fact, only minor exterior modifications were made in order to improve fitting of the part in the snowmobile as well as facilitate its assembly. Some examples of the improvements implemented include, but are not limited to: dimension constrains, substitution of wide radius bends for simple bends, addition of bends in some strategic points in order to limit welding, etc. The biggest alteration to the design is the fact that the front panel is now removable. This allowed us, during testing period, to properly examine the quality of the absorbent material used; improper isolation was a major flaw we encountered during last year's competition. The following figures compare the previous version of the muffler with the new one.

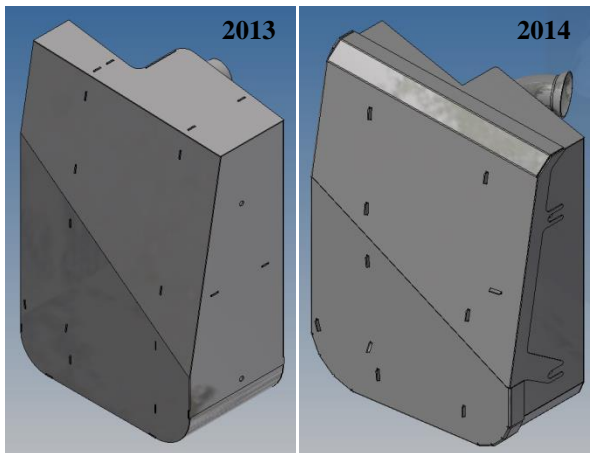


Figure 9 and 10 –New and Old Exhaust Muffler Design

The interior of the silencer is also very similar to that of last year's. Exhaust gases follow the same path through the various sections. The only notable modification is the replacement of the pair of resonators parallel to the center tube in the middle section, with three different length resonators fixed vertically to the said center tube. The length of each resonator has been determined experimentally in order to mitigate the desired sound frequencies. This being said, the more present 600Hz, 700Hz and 850Hz are now greatly dampened. Furthermore, the slight design rework allows the elbow at the entry of the muffler to serve as an additional resonator (see arrow in figure 12). Sections 1, 2 and 3 are purposely filled with sound dampening material in order to lessen the noise generated by the entire frequency range. This process performs significantly well with higher frequencies.

Figures 11 and 12 illustrate the interior design of the two latest exhaust designs.

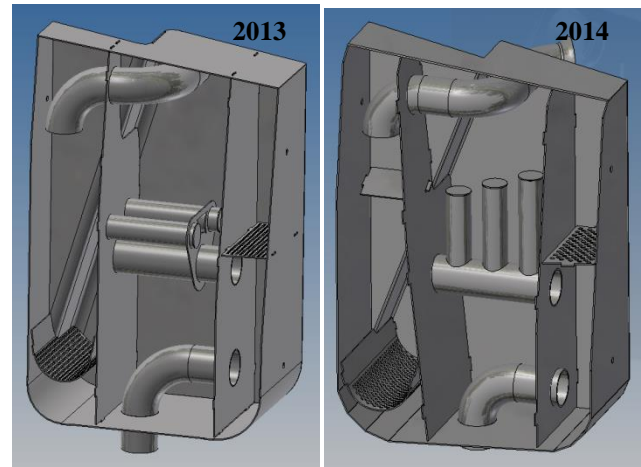


Figure 11 and 12 - Muffler's Interior Design

With the sole purpose of optimising the length of the resonators and reducing noise, many acoustic tests were performed on the motor. These measurements were conducted on an exhaustless engine at various rotation speeds (from 4000RPM to 7000RPM by increments of 500RPM). The 3D graph from figure 19 in the Appendix C points out these results. These results indicate that the engine generates most of its strong frequencies between 150 Hz to 900 Hz. By adjusting the resonator's length, it will be possible to increase the exhaust system's efficiency and eliminate the targeted frequencies.

Resonator length calculation

A simple equation allows us to determine the necessary length of a resonator in order to eliminate the desired frequencies:

$$f = \frac{c}{4 * L} \quad (11)$$

However, in practice there is a phenomenon called *edge effect* which slightly distorts the expected results. Indeed, the edge of a resonator influences the path of a wave in a way that simulates a longer tube length than what it really is. Thus, to counter this deviation, the resonator must be slightly shorter than what the theoretical value suggests. Table 4 in Appendix A shows the difference between speculated theoretical frequencies and experimentally observed frequencies for the resonators present in the exhaust system.

The substantial difference between the expected and obtained results is what encouraged us to modify the sound reduction system of the exhaust. Thereby, we were able to match the desired frequencies by adjusting each resonator's length inside the muffler and therefore increase its efficiency. Appendix B shows the measurements for each resonator. It wasn't possible to experimentally measure the frequency in the resonator at

the entry of the muffler which explains why it wasn't modified.

Final Results

Finally, we ran new tests with the new exhaust fitted to the engine and were able to achieve the results found in the 3D graph from figure 20 in Appendix C. On a global point of view, the noise level is reduced throughout the entire sound stage. Moreover, it seems that engine speed only slightly affects noise intensity. It is nonetheless hard to quantify noise reduction by simply comparing the figure 19 and figure 20. Thus, the figure 13 shows the logarithmic difference between the exhaustless engine and the one fitted with this year's exhaust.

Noise difference between the two mesures (straight and with 2014 exhaust)

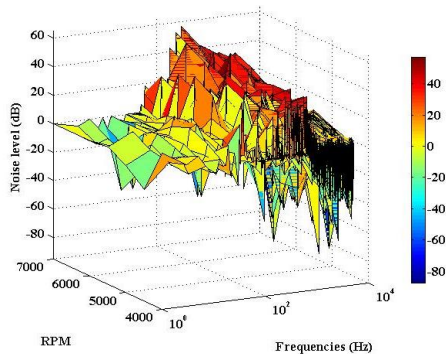


Figure 13 - Noise Reduction from 2014 Exhaust

The exhaust seems to be more effective in the 200 to 1000Hz range, which specifically corresponds to the loudest zone of the sound stage. Therefore, the resonators and absorption chambers have adequately been optimised. However, the major improvement noticed in the 200 Hz range remains unexplained, since our sound reduction methods did not aim this frequency. It would be important and even necessary to push our research a step further in order to understand which element affects this particular frequency.

Track Bench Test and Noise Analysis

For the past years, Club Quiets has successfully designed exhaust systems that reduce noise to a point where the track becomes the major noise source of the snowmobile. With this in mind, the club has decided to build a test bench for which the sole purpose is to study this aspect. The project being established on a long term base, this year's objective was to build the test bench and conduct the first sound tests.

Bench Test Description

The test bench consists mainly of a steel structure that supports the chassis of the snowmobile. It is held by the front suspension mounting points as well as by the rear reinforcement bar. The structure itself is equipped with auto

blocking wheels that allow the bench to be moved around easily. An electric motor is located where the combustion engine usually sits and it drives a belt. A hinge holds the motor in place and uses the weight of the motor to properly tension the belt. Finally, the belt transmits the power directly from the motor to the track's sprocket. Figure 14 shows the test bench while fitted with the transmission system.



Figure 14 - Track Acoustic Bench Test

Acoustic Results

After fabricating and perfecting the test bench, we were able to conduct the first acoustic tests driven solely by the track. It was however important to firstly perform a theoretical analysis of the setup in order to spot the frequencies that should be expected to stand out during the tests. Table 3 presents the said frequencies for a speed of 45 mph at 2100RPM, a typical cruising speed.

Table 3 - Noise Frequencies Caused by Various Components

	Frequency (Hz)
Sprocket	
Rotation	35
Teeth	280
Big wheel (ATV)	
Rotation	25
Big wheel	
Rotation	35
Small wheel	
Rotation	45
Track	
Rotation	7
Pallets	280

The measurements taken this year show the comparison between the BRP manufactured R-Motion suspension with stock 7 inch wheels and the same suspension but with 10 inch wheels fitted instead. As a matter of fact, the team has the

assumption that replacing the wheels of the track with bigger ones might very well help reduce the amount of noise generated by the track while also facilitating its rotation (wider bending radius). This year, the test bench allowed us to verify our hypothesis. The following graph shows the comparison between the two suspension setups in the form of a frequency spectrum.

done is a step forward in the right direction toward the design of an eco-friendly, yet powerful snowmobile.

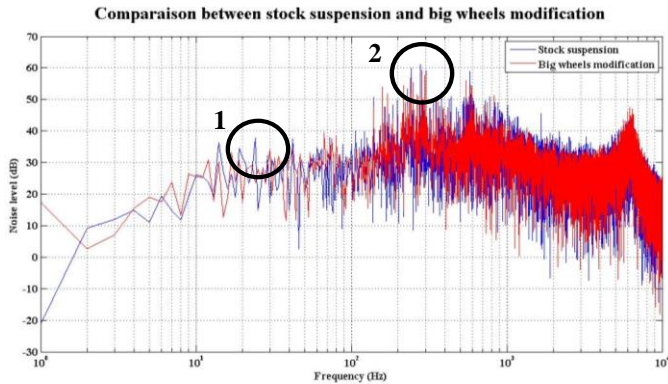


Figure 15- Noise Comparison between 7" and 10" wheels

As we can see on the graph, it appears that the results of both setups are very similar and that there doesn't seem to be any significant difference in terms of noise level. In fact, the noise frequencies that are specifically due to the rear wheels (25 and 35Hz, see table 3) do not seem dominant (circle 1), whereas the noise coming from the movement of the track's pallets is a lot more significant. Nevertheless, it seems that this sound figure remains somewhat identical no matter what wheel setup is used (circle 2).

Thereby, after analysis there seems to be no real advantage in using bigger track wheels to reduce noise. In essence, our efforts should be directed to the sprocket's engagement mechanism, since it is ostensibly one of the noisiest components. Essentially, we are unable to explain many of the dominant frequencies presented in the graph, therefore further research should be addressed to these measurements in order to better understand the frequency spectrum and consequently come up with more noise reduction solutions.

SUMMARY/CONCLUSIONS

The design our new 4-stroke turbocharged engine is a new step for Team QUIETS. Having not a lot of experience with turbo charged engines, we can proudly say that we have successfully implemented one of the first turbocharged 600 ACE with variable engine mapping. The implementation of a modified intake manifold, improved exhaust muffler design, simplified wire harness and efficient EGR valve put this sled ahead of stock model regarding efforts to change the image of dirty snowmobiles and changing them. Although we did not have enough time to provide enough concrete results and prove that our theories and modifications worked, we are confident based on preliminary results that the work we have

REFERENCES

1. Çengel, Y.A., Boles, M.A., Lacroix, M.
"Thermodynamique : une approche pragmatique",
Chenelière Edition, 2008
2. Çengel, Y. A. & Cimbala, J. M. 2014 "Fluid Mechanics:
Fundamentals and Applications", 3rd Edition, McGraw-
Hill, New-York.
3. Leventis Y A, Pavalatos I, Abrams R F "1994 Control of
diesel soot hydrocarbon and NOx emissionswith a
particular trap." *SAE Technical Paper* 940460
4. Miller, J. and C. Bowman. "Mechanism and modeling of
nitrogen chemistry in combustion: Prog Energy"
Combustion. *Sci. 15*, 287-338, 1989
5. Willard W. Pulkrabek, «Engineering Fundamentals of the
Internal Combustion Engine», University of Wisconsin:
Prentice Hall

Definitions/Abbreviations

CO	Carbon Monoxide
CO ₂	Carbon Dioxide
EGR	Exhaust Gas Re-circulation
EGT	Exhaust Gas Temperature
EMS	Engine Management System
HC	Hydro Carbon
H ₂ O	Hydrogen Dioxide
Hz	Hertz
MPH	Miles per hour
NO _x	Different groups of nitrous oxides
RPM	Rotations per minute

APPENDIX A

Table 4 - Resonator Length Adjustments

	Length (mm)	Theoretical (Hz)	Experimental (Hz)	Difference (%)
R _{Entry}	95	897,37		
R ₁ (Short)	90	947,22	853	-9,95
R ₂ (Medium)	110	775,00	704	-9,16
R ₃ (Long)	133	640,98	587	-8,42

APPENDIX B

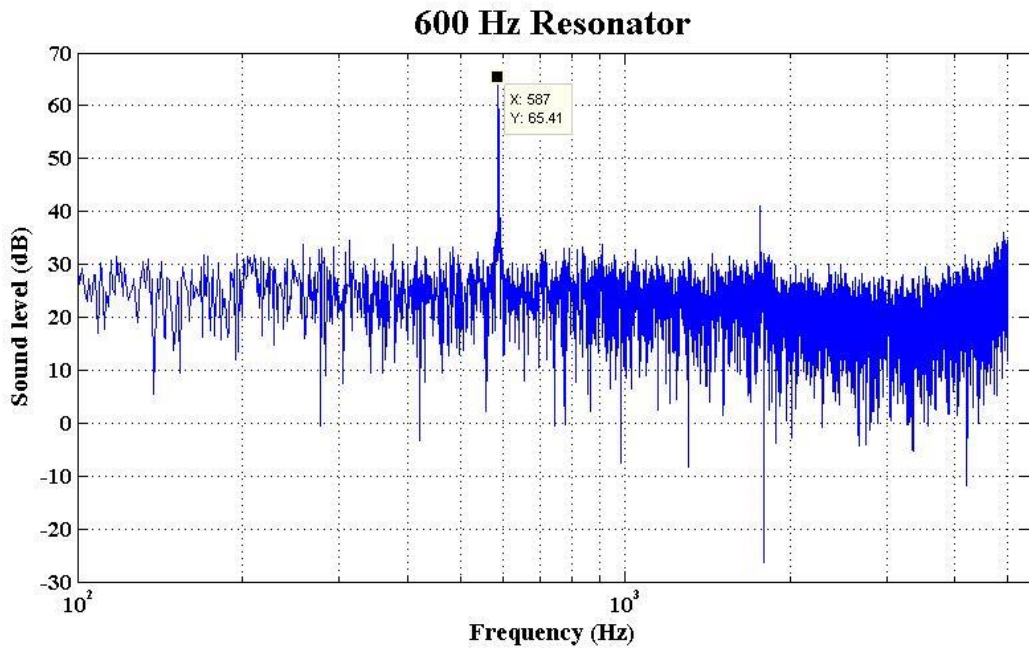


Figure 16 – Resonator for 600 Hz

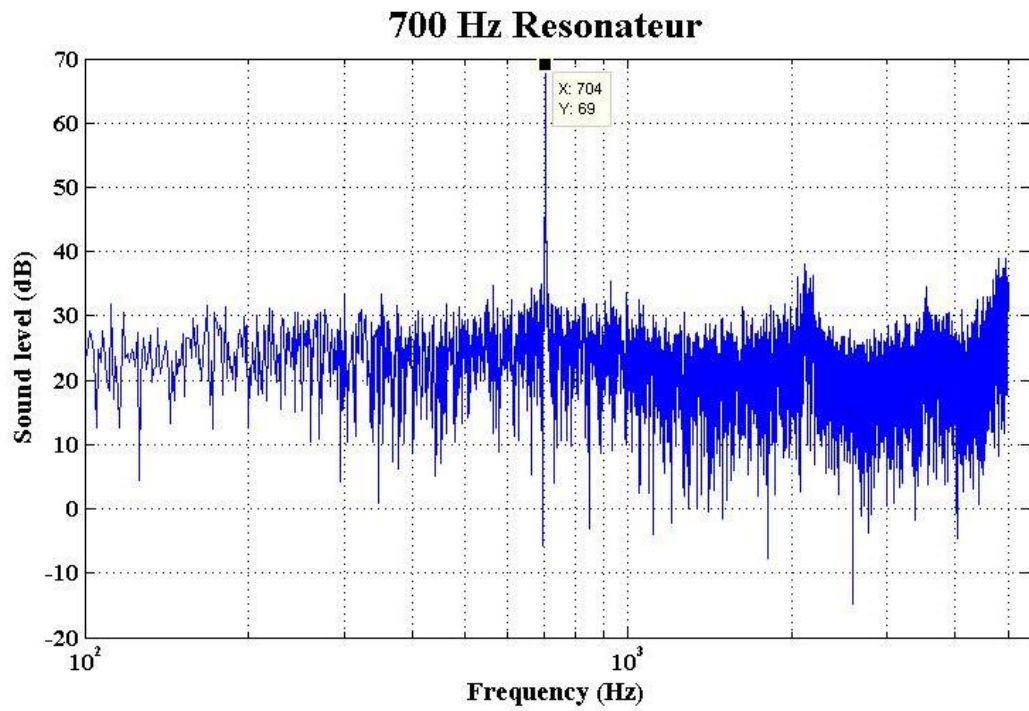


Figure 17 – Resonator for 700 Hz

850 Hz Resonator

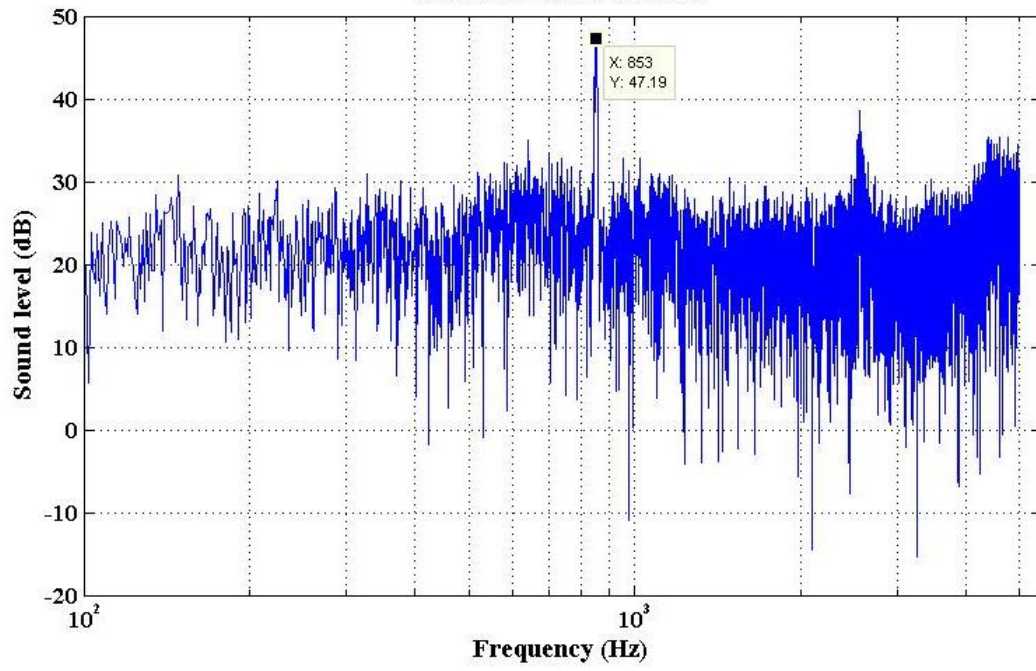


Figure 18 – Resonator for 850 Hz

APPENDIX C

Noise level vs frequencies and RPM (straight)

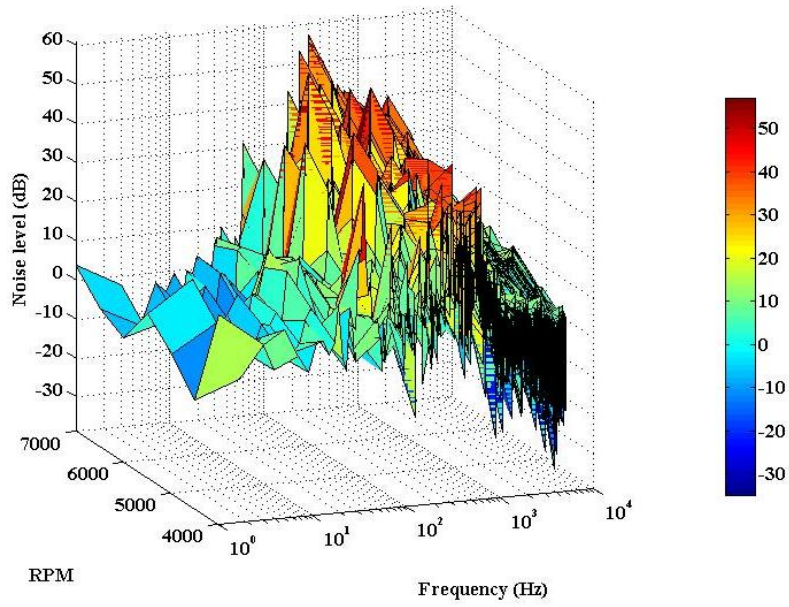


Figure 19 - Engine Noise Level with no Muffler

Noise level vs frequencies and RPM (2014 exhaust)

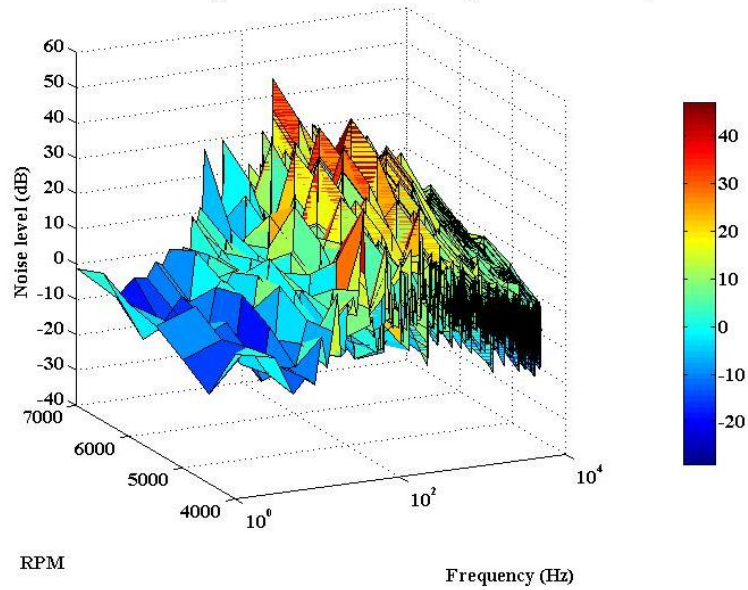


Figure 20 - Engine Noise Level with New 2014 Exhaust System